Original Article

Title: *Fgf20* and *Fgf4* may contribute to tooth agenesis in epilepsy-like disorder mice

Nao Ogawa [a,*], Kunihiko Shimizu [b,c]

[a] Department of Pediatric Dentistry, Nihon University Graduate School of Dentistry at Matsudo, Matsudo Chiba, Japan
[b] Department of Pediatric Dentistry, Nihon University School of Dentistry at Matsudo, Matsudo Chiba, Japan
[c] Nihon University Research Institute of Oral Science, Chiba, Japan

* Corresponding author. Department of Pediatric Dentistry, Nihon University Graduate School of Dentistry at Matsudo, 2-870-1 Sakaecho-Nishi, Matsudo, Chiba 271-8587, Japan.
E-mail address: mana12008@g.nihon-u.ac.jp (N. Ogawa).

Abstract

Background/purpose: Tooth agenesis is one of the most clearly recognized dental anomalies in the permanent dentition and can be challenging to manage clinically. Recent genetic studies identified several genes related to syndromic and nonsyndromic human dental agenesis. However, the genetic factors related to agenesis of the third molars (M3s), second premolars, and lateral incisors, which are most commonly involved in hypodontia, are still unknown. Therefore, this study aimed to identify the genetic causes of the lacking M3s in epilepsy-like disorder (EL) mice, which have 100% incidence of M3 agenesis.

Methods: M3 tooth germs from EL and C57BL/6 control mice on postnatal day 3 were dissected out and total RNA was extracted. mRNA expressional analysis was carried out using DNA microarray, real-time polymerase chain reaction and *in-situ* hybridization.

Results: DNA microarray analysis revealed significantly decreased expression of *Fgf20* and *Fgf4* and increased expression of *Eda* in the M3s of EL mice at the bud stage relative to C57BL/6 control mice, which was supported with both reverse-transcriptase polymerase chain reaction and quantitative real-time polymerase chain reaction analyses ($p < 0.05$). Furthermore, *in-situ* hybridization revealed low mRNA expression levels of *Fgf20* and *Fgf4* in the M3s of EL mice, whereas strong signals were observed in control mice.

Conclusion: Our results suggest that a decrease of *Fgf20* and *Fgf4* expression may lead to M3 agenesis in EL mice. Understanding the mechanisms controlling tooth agenesis will facilitate the development of strategies for tooth bioengineering.

Keywords: gene expression, hypodontia, *in-situ* hybridization, tooth agenesis

Introduction

Tooth agenesis is the most common developmental anomaly of the human dentition. The prevalence of agenesis of the permanent dentition, excluding the third molars (M3s), ranges from 1.6% to 9.6% in the worldwide population [1]. The M3s are missing most frequently, affecting up to 20% of the population, followed by the mandibular second premolars, maxillary lateral incisors, and maxillary second premolars [2,3]. The misalignment, malocclusion, and oral functional problems caused by tooth agenesis in childhood emphasize the importance of understanding the primary causes. Congenital tooth agenesis is characterized by failure of tooth development during tooth organogenesis. More than 150 syndromes are currently known to be related to tooth agenesis [4]. In previous studies, candidate gene mutations in *Msx1* [5], *Pax9* [6], *Axin2* [7], *Wnt10a* [8], *Spry2*, *Spry4* [9], and the ectodermal dysplasia genes *Eda* [10] have been associated with nonsyndromic tooth agenesis. In most cases of tooth agenesis, the causes remain unknown, indicating that additional genes must be involved [11–13].

Although the causes of M3 or incisor-premolar hypodontia in humans are still unknown, mice have high genetic and chromosomal homology with humans. Thus, isolating the genetic cause of hypodontia in mice may suggest a candidate gene in a homologous region for tooth agenesis in humans. Congenital tooth agenesis is seldom observed in inbred mouse strains: the reported frequency of M3 absence is 18% for CBA/Gr mice [14], 3% for CBA/J mice, and 2% for A/J mice [15]. About 92–100% in mutant stocks such as *tabby* [16], *downless*, and *crinkled* [17] mice affect tooth morphological structure and M3 absence. However, in such mutants, the absence of M3 is part of the pleiotropic phenotypes that are analogous to human hypohidrotic ectodermal dysplasia. Epilepsy-like disorder (EL) mice were established as an animal model for studying epilepsy [18] and

evince 100% incidence of M3 agenesis without any generalized craniofacial anomalies [19]. EL mice therefore may be a good model for genetic studies of M3 agenesis or other types of tooth agenesis in humans. Herein, we employed EL mice to identify candidate genes for tooth agenesis.

Materials and methods

Animals

EL mice were obtained from the Laboratory Animal Resource Bank at the National Institute of Biomedical Innovation (Osaka, Japan). C57BL/6 mice were obtained from Japan SLC, Inc. (Shizuoka, Japan). All animals were kept and used according to the guidelines of the Nihon University Intramural Animal Use, Matsudo Chiba, Japan. The experimental protocol was approved by the Nihon University Institutional Animal Experiment Committee (No. AP11MD029).

Frequency of M3 absence

EL and C57BL/6 mice were killed under deep anesthesia with CO_2 at 8 weeks of age. The heads were soaked in 1% KOH at 42°C for 24 hours, and the soft tissue was removed. The upper and lower M3s were observed under a dissection microscope.

Histological examination

The heads of EL and C57BL/6 mice were fixed in 10% paraformaldehyde for 24 hours, embedded in paraffin, and cut into sections (10 μm). Sections were stained with hematoxylin and eosin. The histopathological changes of M3s on postnatal day 3, postnatal day 4, and postnatal day 5 were observed using light microscopy.

4

RNA extraction

Development of the M3 tooth germ of EL mice stops in the bud stage on postnatal day 3. Ten EL mice and 10 C57BL/6 mice were killed under anesthesia, and their heads were immediately embedded in Tissue-Tek compound (Sakura Finetechnical Co., Ltd., Tokyo, Japan). Tissue sections (30 μm) for freezing were prepared using a LeicaCM1520 (Leica Microsystems, Wetzlar, Germany). Sections were stained with 0.25% toluidine blue for 10 seconds. M3 tooth germs were dissected from the upper and lower jaws using a needle under a dissecting microscope, avoiding the tissues surrounding the tooth follicle. A total of 40 M3s from each strain were collected and stored in RNA*later*® RNA Stabilization Reagent (Qiagen, Tokyo, Japan). Total RNA was extracted from sections with an RNeasy® Mini kit (Qiagen), according to the manufacturer's instructions. The quantity of RNA was measured using a spectrophotometer (NanoDrop™ 2000c; Thermo Fisher Scientific, Kanagawa, Japan), and the integrity of the RNA was confirmed by using an Agilent 2100 Bioanalyzer (Agilent Technologies, Foster City, CA, USA).

Microarray hybridization

Microarray hybridization was performed with RNA according to the Agilent Expression Array protocols. The RNA was labeled with Cy3 using a SureTag Complete DNA Labeling Kit (Agilent Technologies) and hybridized on the microarray (SurePrint G3 Mouse GE Microarray; 8 × 60 K, 39,430 Entrez Gene RNAs) using a Gene Expression Hybridization Kit (Agilent Technologies) according to the manufacturer's instructions. After hybridization, the slide glass was washed using Gene Expression Wash Pack (Agilent Technologies), and the images were scanned using a SureScan Microarray Scanner (Agilent Technologies). Fluorescence intensity was calculated using an Agilent Feature Extraction Software (Version 11.5.1.1, Agilent Technologies), and data analysis was

performed using the GeneSpring GX13 software (Agilent Technologies). These background-corrected intensities between arrays were normalized to an average intensity of 2,500 with manufacturer-defined parameters.

Reverse-transcription polymerase chain reaction

The PCR primers of *Fgf20*, *Fgf4*, and *Eda* were designed based on Ensembl (http://asia.ensembl.org/index.html) (Table 1). A glyceraldehyde-3-phosphate dehydrogenase gene (*GAPDH*) was used as an internal control. Total RNAs (100 ng) from tooth germs of M3s of EL mice and C57BL/6 mice were reverse-transcribed into complementary DNA (cDNA) with a PrimeScript High Fidelity RT-PCR kit (Takara, Tokyo, Japan). The PCR conditions were as follows: initial denaturation at 94°C for 5 minutes followed by 35 cycles of 94°C for 30 seconds, 60°C for 30 seconds, and 72°C for 30 seconds in the GeneAmp® PCR System 9700 (Applied Biosystems, Tokyo, Japan). The products were electrophoresed using 2% agarose gel and analyzed.

Quantitative real-time PCR

Real-time PCR was carried out with Thermo Scientific DyNAmo SYBR Green qPCR kits (Thermo Fisher Scientific, Kanagawa, Japan). The sequences of the primers for real-time PCR were the same as those used for RT-PCR. *GAPDH* was used as an internal control. The PCR conditions were as follows: initial denaturation at 95°C for 5 minutes followed by 40 cycles of 94°C for 30 seconds, 60°C for 30 seconds, and 72°C for 30 seconds in the DNA Engine OPTICON Continuous Fluorescence Detector (Bio-Rad, Hercules, CA, USA). The fluorescence level was measured over time. The levels relative to *GAPDH* mRNA in each sample were calculated from standard curves obtained by sequential dilution of total RNA extracted from the heads of C57BL/6 mice at postnatal day 3. Statistical differences between EL and C57BL/6 mice were analyzed from five experiments

using the nonparametric Mann-Whitney *U* test. Values of *p* < 0.05 were considered significant.

In situ hybridization

In situ hybridization targeting *Fgf20* and *Fgf4*, as noted above, was performed according to the Genostaff protocol (Tokyo, Japan). Tissue sections were embedded in paraffin and rehydrated through an ethanol series and phosphate-buffered saline (PBS). The sections were fixed with 10% formalin in PBS for 15 minutes and then washed with PBS. The sections were treated with 4 µg/mL proteinase K in PBS for 10 minutes at 37°C, washed with PBS, refixed with 10% neutral buffered formalin for 15 minutes, again washed with PBS, and placed in 0.2N HCl for 10 minutes. After washing with PBS, the sections were placed in 1 × G-Wash (Genostaff). RNA probes were designed from the mouse *Fgf20* cDNA (NM_030610.2; sequence position 22-335) and *Fgf4* cDNA (NM_010202.5; sequence position 1034-1647). The RNA probes were labeled with digoxigenin (DIG; Roche Molecular Biochemicals, Mannheim, Germany). Hybridization was performed with 300 ng/mL probes in G-Hybo (Genostaff) for 16 hours at 60°C. After hybridization, the sections were washed in 1 × G-Wash for 10 minutes at 60°C and then 50% formamide in 1 × G-Wash for 10 minutes at 60°C, twice with 1 × G-Wash for 10 minutes at 60°C, twice with 0.1 × G-Wash for 10 minutes at 60°C, and twice with 0.1% Tween-20 in Tris-buffered saline (TBST). After treatment with 1 × G-Block (Genostaff) for 15 minutes, the sections were incubated with anti-digoxigenin alkaline phosphatase conjugate (Roche Diagnostics, Basel, Schweiz) and diluted 1:2000 with 50 × G-Block (Genostaff) in TBST for 1 hour. The sections were washed twice with TBST and incubated in 100mM NaCl, 50mM $MgCl_2$, 0.1% Tween-20, and 100mM Tris-HCl, pH 9.5. Coloring reactions were performed with nitro-blue tetrazolium/5-bromo-4-chloro-3-indolyl-phosphate solution (Sigma-Aldrich Co., LLC., St. Louis, IL, USA) overnight and then washed with PBS. Finally, the sections were counterstained with Kernechtrot stain solution (Muto Pure Chemicals Co., Ltd., Tokyo,

Japan) and mounted with G-Mount (Genostaff).

Mutational analysis

To analyze mutations in the coding sequence of *Fgf20, Fgf4*, and *Eda*, all exons (1-3 of *Fgf20*, 1-3 of *Fgf4,* and 1-8 of *Eda*) from both EL mice and C57BL/6 mice were amplified with PCR. Primers used for this analysis were listed in Table 2. PCR products were directly sequenced by using an ABI Prism 3130xl Genetic Analyzer (Applied Biosystems) with a BigDye Terminator version 3.1 sequencing kit (Applied Biosystems). Sequences obtained were verified against the sequences in Ensembl (*Fgf20*; ENSMUSG00000034014, *Fgf4*; ENSMUSG00000060336, *Eda*; ENSMUSG00000113779).

Results

Frequency of M3 absence

Frequency of M3 absence in both EL mice and C57BL/6 mice was listed in Table 3. M3s were absent in 100% of EL mice. No absence was observed in C57BL/6 mice.

Histological examination

Hematoxylin and eosin staining showed that the development of the M3 tooth germ in EL mice arrested in the bud stage, but its development in C57BL/6 mice progressed to the cap stage (Figure 1).

Microarray hybridization

We selected 137 genes related to tooth from the National Center for Biotechnology Information Database using keywords of teeth/tooth from our microarray results. Then, genes had at least two-fold lower expression in EL M3s than in the control were extracted. Nine per 137 genes were chosen and listed in Table 4. The expressions ratio of *Fgf20* and *Fgf4* were -8.06 and -4.86, respectively. The *Eda* slightly increased ($\log_2$ ratio = 0.29) in EL M3s (Table 4). No difference greater than two-fold was noted in human hypodontia-related genes (*Msx1*, *Pax9*, *Axin2*, *Wnt10a*, *Spry2*, and *Spry4*).

RT-PCR and quantitative real-time PCR

The DNA microarray results revealed interesting expression patterns for *Fgf20* and *Fgf4*. We also examined *Eda*, which has been reported to regulate the expressions of *Fgf20* and *Fgf4* in early development. Therefore, we designed primers for RT-PCR analysis of *Fgf20*, *Fgf4*, and *Eda* (Table 1). To confirm the gene expressions of *Fgf20*, *Fgf4*, and *Eda* from DNA microarray results, RT-PCR analysis was performed. PCR band densities of *Fgf20* and *Fgf4* in M3s of EL mice were lower than those in C57BL/6 mice, whereas *Eda* in M3s of EL mice was higher than C57BL/6 mice (Figure 2A). Further quantification of the mRNA levels of *Fgf20, Fgf4,* and *Eda* was performed using real-time PCR. Significant decreases were detected in *Fgf20* and *Fgf4* mRNA expression levels in M3s of EL mice compared to those of C57BL/6 mice, whereas a significant increase was detected in *Eda* ($p <$ 0.05; Figure 2B).

In situ hybridization

We carried out comparative *in situ* hybridization analysis of M3s from EL mice and C57BL/6 mice in the bud stage at postnatal day 3. *Fgf20* and *Fgf4* were expressed strongly at the tips of bud epithelia of M3s from C57BL/6 mice, whereas little expressions of the *Fgf20* or *Fgf4* in the M3

9

tooth germs of EL mice (Figure 3). Hematoxylin and eosin staining showed that accumulation of the cell of enamel knot at the tips of bud epithelia of M3s from C57BL/6 mice, whereas staining does not showed in EL mice (Figure 3).

Mutational analysis

We identified one silent mutation that does not change the amino acid sequence, in exon 2 of *Fgf4* (c.402C > A, rs32113273) in EL mice. We also identified one nonsynonymous mutation in exon 1 of *Fgf20* (c.52A > G, rs33026537). These sequence variants are all included in the Ensembl cDNA Report.

Discussion

Tooth morphogenesis is regulated by sequential and reciprocal interactions between the oral epithelium and mesenchyme. Morphologically, tooth development starts as a thickening of the oral epithelium. During the subsequent bud, cap, and bell stages, the shape of the tooth is established by epithelial folding morphogenesis in mice [20]. A previous study found that many transcription factors and signaling molecules involved in the *Bmp*, *Wnt*, *TNF*, *Shh*, and *Fgf* pathways regulate tooth development [21]. Fgf, fibroblast growth factor, signaling plays essential roles in regulating many biological processes, including almost all structure development of many craniofacial regions from early patterning to growth regulation and tooth development [22]. Twenty-two Fgf ligands have been identified in mammals, but the role of Fgf signaling is incompletely understood in murine tooth development despite evidence for the involvement of Fgf signaling in odontogenesis [20,23,24]. In this study, we observed low mRNA expression levels of *Fgf20* and *Fgf4* in EL M3s at the bud stage,

suggesting their relationship to M3 agenesis in EL mice.

$Fgf4$ plays a role in embryonic development [25], and homozygotes for targeted null mutations of $Fgf4$ die shortly after implantation whereas conditional mutations show normal development [26]. The importance of $Fgf4$ in odontogenesis has been shown in $Lef1^{-/-}$ mice, which have arrested tooth development. In cultured tooth germ, recombinant FGF4 protein fully overcomes the developmental arrest of $Lef1^{-/-}$ tooth germs, suggesting that $Fgf4$ is essential for tooth development [27].

$Fgf20$ is expressed in both embryonic and adult tissues and is a critical factor in brain development and cell homeostasis [28]. In tooth development, $Fgf20$ directly affects the tooth epithelium, similar to $Fgf4$, which was the first Fgf discovered in the enamel knot [25]. The importance of $Fgf20$ in tooth development has been further shown in the ectodysplasin (Eda) pathway. Eda is a tumor necrosis factor family member that was first identified by positional cloning of the gene for human X-linked hypohidrotic ectodermal dysplasia, a congenital morphogenetic disorder affecting the development of teeth, hair, and exocrine glands [29]. Eda-responsive genes were analyzed with microarray analysis to uncover the developmental functions of the Eda pathway in ectodermal organogenesis, and Eda-induced genes included components of all major growth factor pathways, such as Wnt, Egf, Tnf, and Fgf [30]. Eda regulates and integrates various pathways essential for tooth development, and missense mutations in Eda have been associated with nonsyndromic tooth agenesis in humans [10]. Eda affects Fgf signaling in craniofacial patterning and growth, and one of the functions of Eda in tooth development is to sustain and/or balance the Fgf signaling loop [13]. Eda was previously shown to rapidly induce $Fgf20$ expression, and its activity correlated with the expression levels of $Fgf20$ in vivo [31]. $K14\text{-}Eda;Fgf20^{\beta Gal/\beta Gal}$ mice ($Fgf20$-null mice overexpressing Eda) have smaller molars than wild-type mice, and analysis of tooth morphogenesis in $K14\text{-}Eda;Fgf20^{\beta Gal/\beta Gal}$ mice indicated that $Fgf20$ has an essential function in the Eda-mediated activator-inhibitor balance regulating tooth development [31]. Interestingly, 31%

of *K14-Eda;Fgf20^{βGal/βGal}* mice showed missing M3s, suggesting that lack of *Fgf20* combined with *Eda* overexpression affects M3 agenesis. In our study, real-time PCR analysis showed strong expression of *Eda* in EL M3s compared with controls. Our results suggested that the decrease in *Fgf20* under the overexpression of *Eda* in M3s at the bud stage may relate to agenesis of M3s in EL mice.

Signals from the enamel knot, a morphologically distinct region of the epithelium containing densely packed nonproliferating cells, affect both epithelial and mesenchymal cells, and interactions between the mesenchyme and epithelium are responsible for epithelial morphogenesis during the cap and bell stages [32]. Tooth shape may be regulated by signaling in the enamel knots, and enamel knot activity is mediated, at least in part, by *Fgf4* and *Fgf9* signaling molecules [33]. Morphologically, the enamel knots are first seen at the tips of the tooth bud in the cap stage [32], and *Fgf20* and *Fgf4* expression in the enamel knot was previously demonstrated by *in-situ* hybridization [23,25]. The results of the our study indicating a lack of *Fgf20* and *Fgf4* expression in the M3s of EL mice thus suggest that enamel knots were not formed.

In our mutation analysis, we found nonsynonymous mutation in the exon of *Fgf20* in EL. This mutation has already been registered as rs33026537 single nucleotide polymorphism, and the regulation is unknown. Our result suggests that a new gene mutation is not responsible for M3 agenesis in EL mice. However, the 5′-untranslated region and 3′-untranslated region of *Fgf20*, *Fgf4*, and *Eda* were not analyzed; therefore, we cannot rule out causative polymorphisms of the missing M3s in these regions.

Based on our gene expression analysis, we conclude that low mRNA expression of *Fgf20* and *Fgf4* may contribute to agenesis of M3s in EL mice. These findings provide a basis for further research into the underlying genetic cause of tooth agenesis toward more effective clinical treatment.

Conflicts of interest

The authors declare that no conflict of interest exists.

Acknowledgments

References

[1] Mitsui SN, Yasue A, Masuda K, et al. Novel PAX9 mutations cause non-syndromic tooth agenesis. J Dent Res 2014;93:245–9.

[2] Sarkar T, Bansal R, Das P. Whole genome sequencing reveals novel non-synonymous mutation in Ectodysplasin A (EDA) associated with non-syndromic X-linked dominant congenital tooth agenesis. PLoS ONE 2014;9:e106811.

[3] Endo T, Sanpei S, Komatsuzaki A, et al. Patterns of tooth agenesis in Japanese subjects with bilateral agenesis of mandibular second premolars. Odontology 2013;101:216–21.

[4] Yin W, Bian Z. The gene network underlying hypodontia. J Dent Res 2015;94:878–85.

[5] Vastardis H, Karimbux N, Guthua SW, et al. A human MSX1 homeodomain missense mutation

causes selective tooth agenesis. Nat Genet 1996;13:417–21.

[6] Stockton DW, Das P, Goldenberg M, et al. Mutation of PAX9 is associated with oligodontia. Nat Genet 2000;24:18–9.

[7] Lammi L, Arte S, Somer M, et al. Mutations in AXIN2 cause familial tooth agenesis and predispose to colorectal cancer. Am Hum Genet 2004;74:1043–50.

[8] Kantaputra P, Sripathomsawat W. WNT10A and isolated hypodontia. Am J Med Genet A 2011;155A:1119–22.

[9] Alves-Ferreira M, Pinho T, Sousa A, et al. Identification of genetic risk factors for maxillary lateral incisor agenesis. J Dent Res 2014;93:452–8.

[10] Tao R, Jin B, Guo S.Z, et al. A novel missense mutation of the *EDA* gene in a Mongolian family with congenital hypodontia. J Hum Genet 2006;51:498–502.

[11] Tallón-Walton V, Manzanares-Céspedes MC, Carvalho-Lobato P, et al. Exclusion of PAX9 and MSX1 mutation in six families affected by tooth agenesis. A genetic study and literature review. Med Oral Patol Oral Cir Bucal 2014;19:e248–254.

[12] Arte S, Parmanen S, Pirinen S, et al. Candidate gene analysis of tooth agenesis identifies novel mutations in six, genes and suggests significant role for WNT and EDA signaling and allele combinations. PLoS One 2013;8:e73705.

[13] Lan Y, Jia S, Jiang R. Molecular patterning of the mammalian dentition. Semin Cell Dev Biol 2014;25–6:61–70.

[14] Grüneberg H. The genetics of a tooth defect in the mouse. Proc R Soc B 1951;138:437–51.

[15] Murai M. A genetic study on the development of the lower molars and mandible in mice: Change of genetic and environmental effects in the course of pre-and postnatal morphogenesis. Jpn J Genetics 1975;50:73–90. [In Japanese].

[16] Pispa J, Jung HS, Jernvall J, et al. Cusp patterning defect in Tabby mouse teeth and its partial

rescue by FGF. Dev Biol 1999;216:521–34.

[17] Headon DJ, Emmal SA, Ferguson BM, et al. Gene defect in ectodermal dysplasia implicates a death domain adapter in development. Nature 2001;414:913–6.

[18] Imaizumi K, Nakano T. Mutant stocks, strain El. Mouse News Letter 1964;31:57.

[19] Asada Y, Shimizu T, Matsune K, et al. Absence of the third molars in strain EL mice. Ped Dent J 2000;10:19–22.

[20] Thesleff I. Epithelial-mesenchymal signaling regulating tooth morphogenesis. J Cell Sci 2003;116:1647–8.

[21] Thesleffa I. The genetic basis of tooth development and dental defects. Am J Med Genet A 2006;140:2530–5.

[22] Nie X, Luukko K, Kettunen P. FGF signaling in craniofacial development and developmental disorders. Oral Dis 2006;12:102–11.

[23] Porntaveetus T, Otsuka-Tanaka Y, Basson MA, et al. Expression of fibroblast growth factors (Fgfs) in murine tooth development. J Anat 2011;218:534–43.

[24] Klein OD, Lyons DB, Balooch G, et al. An FGF signaling loop sustains the generation of differentiated progeny from stem cells in mouse incisors. Development 2008;135:377–85.

[25] Niswander L, Martin GR. *Fgf*-4 expression during gastrulation, myogenesis, limb and tooth development in the mouse. Development 1992;114:755–68.

[26] Feldman B, Poueymirou W, Papaioannou VE, et al. Requirement of FGF-4 for postimplantation mouse development. Science 1995;267:246–9.

[27] Kratochwil K, Galceran J, Tontsch S, et al. FGF4, a direct target of LEF1 and Wnt signaling, can rescue the arrest of tooth organogenesis in Lef1(-/-) mice. Genes Dev 2002;16:3173–85.

[28] Grothe C, Timmer M, Scholz T, et al. Fibroblast growth factor-20 promotes the differentiation of Nurr1-overexpressing neural stem cells into tyrosine hydroxylase-positive neurons. Neurobiol Dis

2004;17:163–70.

[29] Kere J, Srivastava AK, Montonen O, et al. X-linked anhidrotic (hypohidrotic) ectodermal dysplasia is caused by mutation in a novel transmembrane protein. Nat Genet 1996;13:409–16.

[30] Lefebvre S, Fliniaux I, Schneider P, et al. Identification of ectodysplasin target genes reveals the involvement of chemokines in hair development. J. Invest Dermatol 2012;132:1094–102.

[31] Häärä O, Harjunmaa E, Lindfors PH, et al. Ectodysplasin regulates activator-inhibitor balance in murine tooth development through Fgf20 signaling. Development 2012;139:3189–99.

[32] Thesleffa I, Sharpe P. Signaling networks regulating dental development. Mech Dev 1997;67:111–23.

[33] Klein OD, Minowada G, Peterkova R, et al. Sprouty genes control diastema tooth development via bidirectional antagonism of epithelial-mesenchymal FGF signaling. Dev Cell 2006;11:181–90.

Captions

Figure 1. The third molar in epilepsy-like disorder (EL) mice and C57BL/6 mice at postnatal day 3 (P3), P4, and P5 (frontal section).

In EL mice, tooth development arrested at P3 but progressed past P3 in C57BL/6 mice. Scale bar, 100 µm.

Figure 2. mRNA expressions of *Fgf20*, *Fgf4*, and *Eda* in the third molars in the bud stage at postnatal day 3.

Reverse-transcription PCR of *Fgf20*, *Fgf4*, *Eda*, and *GAPDH*. Gene expressions of *Fgf20*, *Fgf4*, and *Eda* were observed with that of *GAPDH* on the agarose gel (A). In addition, their mRNA expressions relative to that of *GAPDH* were expressed as the mean ± standard deviation of five experiments (B). * $p < 0.05$.

Figure 3. *In-situ* hybridization with *Fgf20* or *Fgf4* probe in the third molars in the bud stage at postnatal day 3.

Fgf20 and *Fgf4* were preferentially expressed in the third molars of C57BL/6 mice, whereas little expression was noted in EL mice. Scale bar, 50 µm.

HE ; hematoxylin and eosin.

Table 1. Primers for reverse-transcriptase polymerase chain reaction and quantitative real-time PCR.

Gene	Forward/Reverse Primer (5′→3′)	Size (bp)	Region
Fgf20	F; GTGGACAGTGGCCTGTACCT	203	Exon 1
	R; CTGGCACCATCTCTTGGAGT		Exon 2
Fgf4	F; GTGCCTTTCTTTACCGACGA	155	Exon 2
	R; ACCTTCATGGTAGGCGACAC		Exon 3
Eda	F; GGCTCTTCCTGGGTTTCTTT	152	Exon 1
	R; AAGGCTGCTGTTGAAAGGAC		Exon 2
GAPDH	F; GGAAGCCCATCACCATCTTC	203	Exon 1
	R; CGTGGTTCACACCCATCACA		Exon 2

Table 2. Primers for mutational analysis.

Gene	Forward primer (5'→3')	Reverse primer (5'→3')	Region
Fgf20	CAATCTAAGAGGGTGCACTG	ATTCCCTTCTGCCAGGGTGG	Exon1
	GGTAGAGTCGCAGAAGACCA	AAGGCCAGGTGCAATTGTAG	Exon2
	CATGGAACACGGGAAAGCTA	CTCCCGTAATATCCTGAACG	Exon3
Fgf4	CTCGCTACTTAGGTCTGTGC	CAGCCTCAGTCTGGGCGCTT	Exon1
	AAGAGGCTTAGAGTCGGAGG	CCTCTGTGACCAACACACAA	Exon2
	CGTGGACTTATCACCTCTTC	CCAAAGAGGTCTGAGCTGCA	Exon3
Eda	AGGACAGTAGTCGCCTGTCA	CTGGAACTTGGCTCTGAGTG	Exon1
	ACATGATAAGAACAGCGGTG	GGTTAGGCTGGAGAAATCCA	Exon2
	GGACCATGACTATGGGCTCC	GATTGAATGAAGCAATGGGC	Exon3
	GAAGTCTCTAGAACTCCCTG	CCTCTACACTAGACTAGGGA	Exon4
	CTCCAGCTGTAAGGCCTGGA	GGGAATCTCATAGGCAAAGG	Exon5
	ATAGCTCAAGACAGAGGGAG	GGAGGAGTTAGGCTGGCTGA	Exon6
	AGATAGGGTTGATGGGGAGG	ATGGTTTTGGCTTGCTCCAC	Exon7
	AGGCACAGTTTCGGGTGGCA	CCACACACAGCAGCACTTAG	Exon8

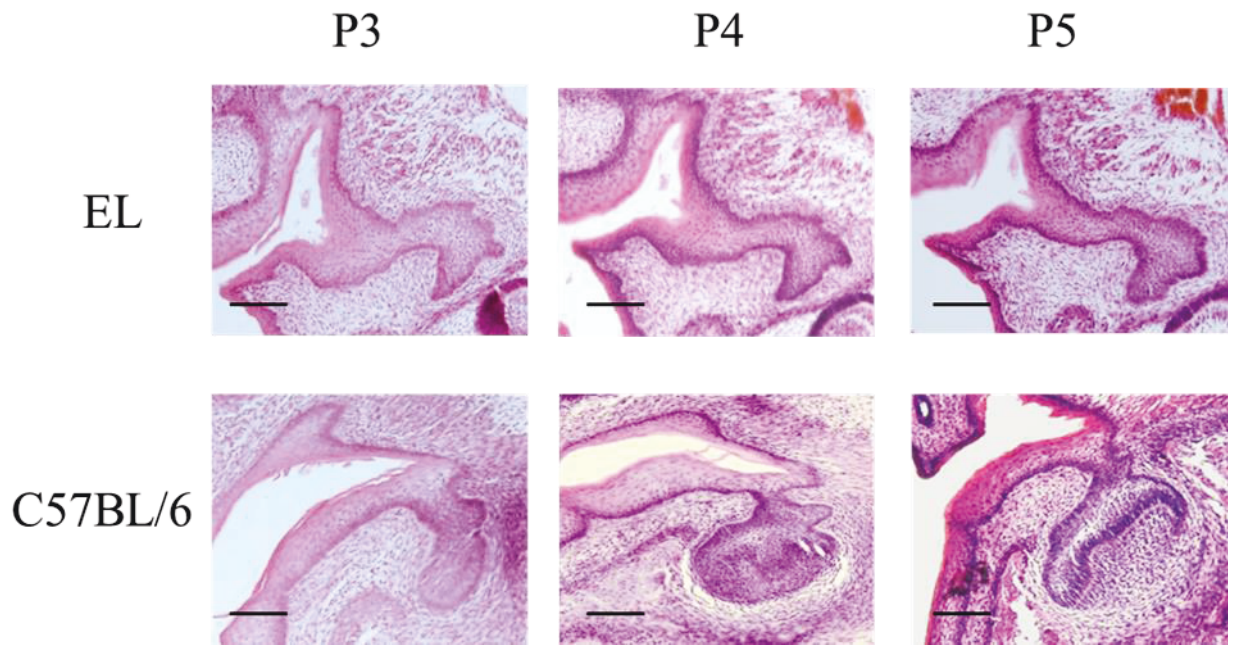**Table 3.** Frequency of third molar absence in epilepsy-like disorder (EL) and C57BL/6 mice.

Strain	No. of mice	Frequency of absence all M3s (%)
EL	16	100
C57BL/6	16	0

M3s = third molars.

Table 4. Gene expression ratios in epilepsy-like disorder (EL) mice compared with C57BL/6 mice by microarray analysis.
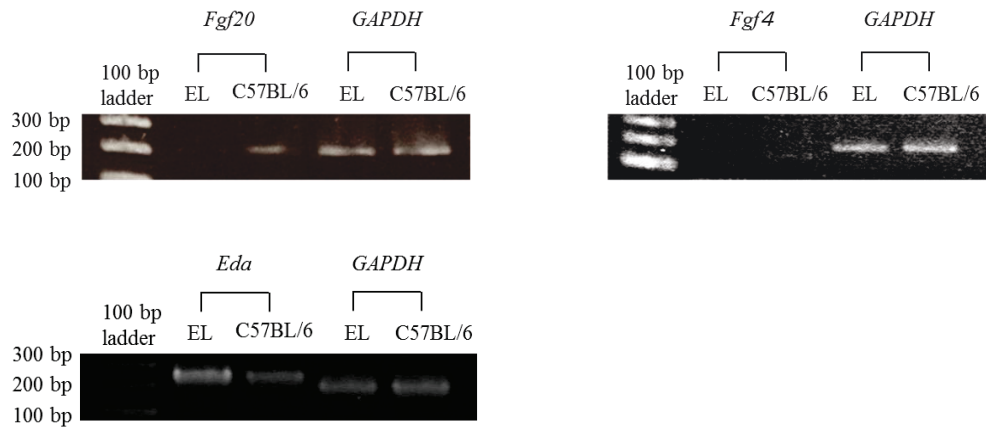
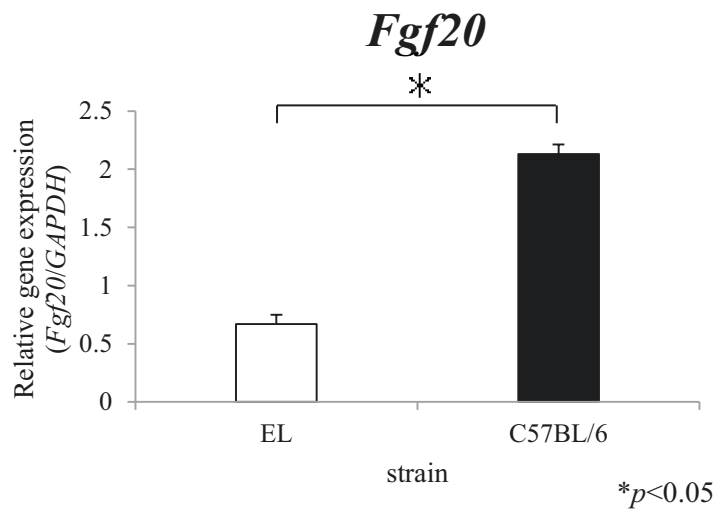| Symbol	Genes related to tooth formation	Ratio
Fgf20	fibroblast growth factor 20	-8.06
Fgf4	fibroblast growth factor 4	-4.86
Fgf2	fibroblast growth factor 2	-4.35
Gnrh1	gonadotropin releasing hormone 1	-3.89
Erbb4	erb-b2 receptor tyrosine kinase 4	-2.36
Hand1	heart and neural crest derivatives expressed transcript 1	-2.20
Lrp4	low density lipoprotein receptor-related protein 4	-2.10
Cdk2ap1	CDK2 (cyclin-dependent kinase 2)-associated protein 1	-2.10
Folr1	folate receptor 1	-2.06

Figure 1
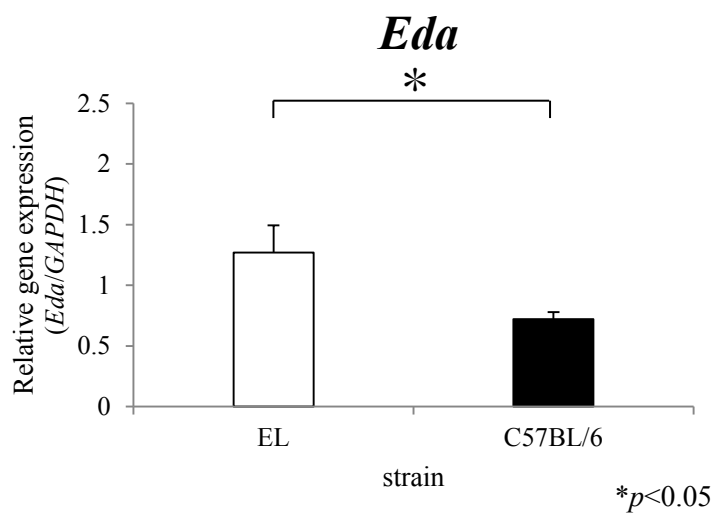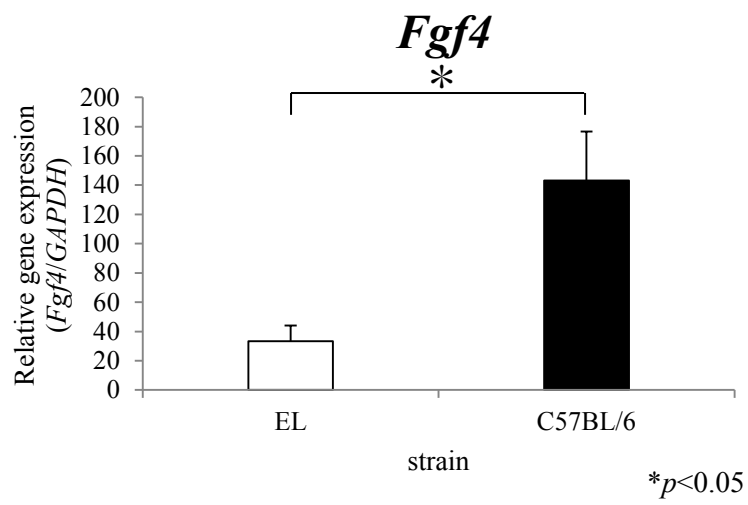
Figure 2

A

B

Fgf4

*p<0.05

Eda

*p<0.05

Figure 3

EL   C57BL/6

HE stain

Fgf20

Fgf4

50 μm   x200